

# Time-resolved, nonperturbative, and off-resonance generation of optical terahertz sidebands from bulk GaAs

M. A. Zudov\* and J. Kono†

*Department of Electrical and Computer Engineering, Rice University, Houston, Texas 77005*

A. P. Mitchell‡

*W. W. Hansen Experimental Physics Laboratory, Stanford University, Stanford, California 94305*

A. H. Chin

*Lawrence Livermore National Laboratory, P. O. Box 808, Mail Stop L-174, Livermore, California 94551*

(Received 3 April 2001; published 6 September 2001)

We have investigated terahertz (THz) sideband generation from bulk GaAs using intense pulses of coherent THz (or far-infrared) radiation from a free electron laser. In contrast to previous studies, sidebands appeared inside the band gap and therefore were not resonantly enhanced from real states. Also, using picosecond pulses and changing the temporal overlap between the THz and near-infrared pulses allowed us to monitor the evolution of the THz sidebands directly in the time domain; this suggests a convenient method for characterizing THz pulses using a conventional Si photodetector. In addition to an expected second-order sideband, we detected a first-order sideband, which has previously been observed only in an asymmetrically coupled double quantum well system where the inversion symmetry was intentionally broken. Finally, the THz power dependence clearly revealed a deviation from perturbative behavior, indicating the entrance into the strong-field regime.

DOI: 10.1103/PhysRevB.64.121204

PACS number(s): 78.20.-e, 78.47.+p

The properties of semiconductors can be drastically modified when they are subjected to an intense external electric field. In particular, intense fields can significantly modify optical properties, leading to various electro-optical phenomena in semiconductors including the Franz-Keldysh effect,<sup>1,2</sup> the quantum confined Stark effect,<sup>3</sup> and the quantum-well Pockels effect.<sup>4</sup> Exploring these strong-field electro-optical effects in high-frequency ac fields, especially in the THz range, is not only important technologically, but also allows us to study new multiphoton, strong-field phenomena that cannot be probed by other traditional methods. This is primarily due to the efficient coupling of the THz electric fields to various intraband excitations in semiconductors, which in turn modify their optical properties.

In this paper, we report on the generation of THz sidebands from a bulk GaAs crystal. In this multiphoton process, a weak optical or near-infrared (NIR) beam passes through a THz-driven semiconductor, acquiring strong emission lines, or optical THz sidebands, with frequencies separated by integer multiples of the THz frequency:

$$\omega_n = \omega_{\text{NIR}} + n\omega_{\text{THz}}; \quad n = \pm 1, \pm 2, \pm 3 \dots \quad (1)$$

It was previously demonstrated<sup>5</sup> that these lines completely dominate the near-bandedge emission properties of THz-driven semiconductors. Recent theoretical studies predicted intriguing phenomena for THz sidebands such as dynamical symmetry breaking,<sup>6</sup> nonmonotonic power dependence,<sup>7</sup> chaotic behavior,<sup>8</sup> sideband disappearance under cyclotron resonance,<sup>9</sup> and THz-induced subband hybridization.<sup>10</sup> However, none of these have been observed to date.

Previous observation of THz sidebands in semiconductors relied on *resonant enhancement* using either magnetoexciton

states<sup>5</sup> or quantum-well subband states.<sup>11</sup> Since the intensity of THz field remained rather weak, the main results were successfully explained by a *perturbation* theory.<sup>12</sup> In the work by Phillips *et al.*<sup>11</sup> the inversion symmetry of the system was intentionally broken, allowing the detection of odd ( $n = \pm 1$ ) sidebands, whereas in the work by Kono *et al.*<sup>5</sup> only even ( $n = \pm 2, \pm 4$ ) sidebands were observed. In either case, presumably due to the resonant nature and smaller intensities used, there was no signature of *bulk*  $\chi^{(2)}$  contribution, which should always exist in zinc-blende semiconductors even with quantum wells grown on top. Finally, both previous studies were essentially continuous wave (CW), and thus did not provide any information on the evolution of the sidebands in the time domain. In this paper, we present results on *time-resolved* spectroscopy of *nonperturbative, off-resonance* THz sideband generation from *bulk* GaAs.

We utilized the unique characteristics of the Stanford Free Electron Laser,<sup>13</sup> i.e., the wide spectral range (5–100 THz or 3–70  $\mu\text{m}$ ), the short pulse duration (0.6–5 ps), and the high peak powers (up to 2 MW). The THz pulse train consisted of “macropulses” with the repetition rate of 5–20 Hz, which, in turn, contained picosecond “micropulses” at 11.8 MHz. The NIR radiation was provided by a regenerative amplifier seeded by a mode-locked Ti:Sapphire laser, which was driven at the seventh harmonic (82.6 MHz) of the micropulse repetition rate (11.8 MHz). Radio frequency (RF) synchronization electronics were used to phase lock the FEL and NIR lasers. The pulse width of the NIR pulses was  $\sim 1$  ps. Timing electronics were used to pick out individual NIR laser pulses, and most measurements were made with a single NIR pulse per FEL macropulse. The temporal overlap between the two beams was adjustable using the synchronization electronics and a delay stage. We spatially combined the THz

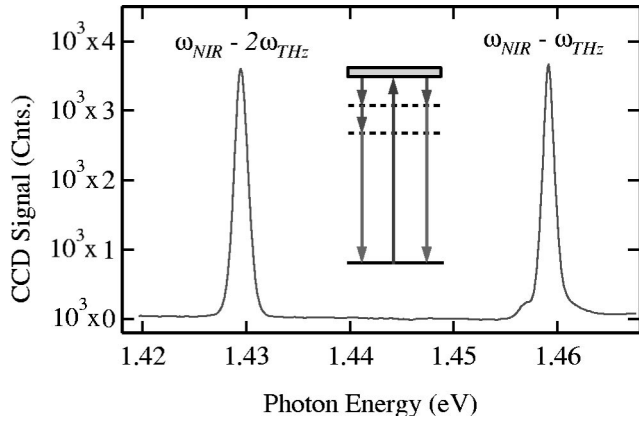


FIG. 1. Typical sideband spectrum at  $\lambda_{NIR}=832$  nm (1.49 eV) and  $\lambda_{THz}=42$   $\mu\text{m}$  (0.03 eV); the inset schematically shows the energy levels in the system involved in the generation of the sidebands. The THz (NIR) intensity used was  $\sim 1 \times 10^8$  ( $1 \times 10^{10}$ )  $\text{W}/\text{cm}^2$ .

pulses with the NIR pulses using a Pellicle plate and then focused the collinear beams onto the sample using an off-axis parabolic mirror down to  $\sim 0.5$  mm. The sample was placed in a He-flow optical cryostat equipped with a variable temperature control ( $T=20\text{--}300$  K). The transmitted and emitted radiation was transported and focused into a NIR spectrometer equipped with a Si CCD. The spectral resolution of the system was  $\sim 1.3$  nm (or 2.6 meV). The spectrometer shutter was controlled by the macropulse trigger, but usually the shutter was left open for a time of many (16–80) macropulses, depending on the signal intensity and the repetition rate. The THz power was monitored *in situ* and averaged during the single acquisition cycle. Most of the measurements were made with the sample rotated along the vertical axis to  $\approx 45^\circ$  with respect to the propagation direction of the incident beams. The polarization of the THz (NIR) beam was usually kept horizontal but could be rotated using a polarizer pair (a half-wave plate). The sample we studied was a (100)-oriented semi-insulating GaAs crystal.

Figure 1 shows a typical sideband spectrum taken at 160 K. As discussed later, this choice of  $T$  allows us to tune the sideband intensities to be approximately equal. Here we observe two lines, which appear precisely at one and two  $\hbar\omega_{THz}$  below the NIR fundamental, i.e., at  $\hbar\omega_{NIR} - \hbar\omega_{THz} = 1.49 - 0.03 = 1.46$  eV and  $\hbar\omega_{NIR} - 2\hbar\omega_{THz} = 1.49 - 0.06 = 1.43$  eV. We therefore identify these lines as the  $\omega_{-1}$  and  $\omega_{-2}$  sidebands, respectively. With our available THz intensities and detector sensitivity, we were not able to detect third- or higher-order sidebands. The energy-level diagram in the inset of Fig. 1 illustrates the experimental situation: the dashed lines are the intermediate *virtual* levels in these parametric processes and the shaded area represents the continuum of real states above the band edge.

There are several features worth pointing out. First, unlike the previous studies,<sup>5,11</sup> the sidebands appear at energies *below* the energy gap  $E_g$ , where there are no real states, and therefore are not resonantly enhanced.<sup>14</sup> Second, we observe an *odd* sideband (i.e., the  $\omega_{-1}$ ) without intentional breaking of the inversion symmetry. We found that the  $\omega_{-1}$  sideband

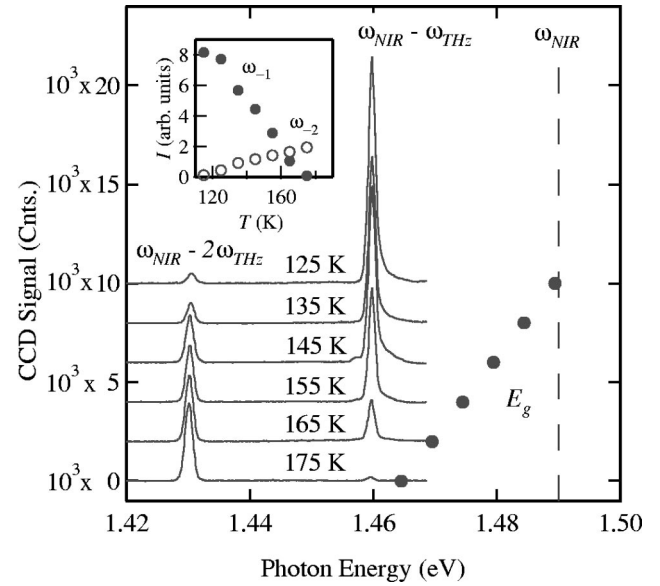


FIG. 2. Sideband spectra at different temperatures. The spectra are offset for clarity. The vertical dashed line denotes the NIR fundamental energy ( $\hbar\omega_{NIR}$ ). The solid circles represent the band gap of the sample as measured by interband absorption spectroscopy for each temperature. Inset: Sideband intensity as a function of temperature. Solid (open) circles represent the experimental values for the  $\omega_{-1}$  ( $\omega_{-2}$ ) sidebands.

depends sensitively on the crystal orientation with respect to the laser beams and their polarization, indicating that its origin is the lack of inversion symmetry of the GaAs crystal. In particular, it disappeared at normal incidence, while the  $\omega_{-2}$  sideband could still be observed. In what follows, we discuss the dependence of the sideband intensity on temperature, the relative delay time between the THz and NIR pulses, and the NIR and THz beam intensities.

In Fig. 2 we show sideband spectra at selected temperatures, which are vertically offset for clarity. The vertical dashed line represents the energy of the fundamental NIR quantum,  $\hbar\omega_{NIR} \approx 1.49$  eV. The solid circles show the band-edge of GaAs for each  $T$ , obtained by interband absorption spectroscopy. As seen from Fig. 2 the intensity of the sidebands is strongly temperature dependent. As  $T$  is raised from 125 to 175 K, the  $\omega_{-2}$  sideband increases in intensity whereas the  $\omega_{-1}$  sideband decreases and eventually vanishes at  $T \approx 180$  K. At higher  $T$  (not shown) the  $\omega_{-2}$  sideband weakens and vanishes at  $T \approx 230$  K. This intriguing behavior is related to the interplay between the absorption of the NIR fundamental and that of the sidebands; i.e., while a larger density of states at the fundamental energy favors more intense sidebands, no real states are desirable at the sideband frequencies, since they will be absorbed. The fact that the  $\omega_{-2}$  sideband persists to higher  $T$  is a direct consequence of its lower energy as compared to the  $\omega_{-1}$  sideband, in agreement with the temperature dependence of the GaAs bandedge. In the remainder of the paper we show data taken only at 160 K, where the sidebands are approximately equal in intensity.

Since we used picosecond THz pulses, we were able to probe the evolution of the THz sidebands directly in the time

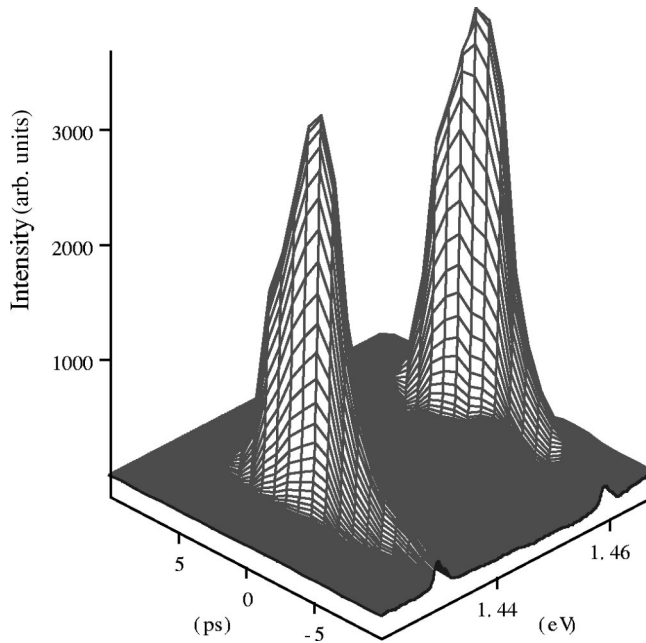


FIG. 3. Sideband intensity as a function of photon energy and relative delay between the NIR and THz pulses. This represents a convenient method for characterizing THz pulses using a Si photodetector.

domain. Using the delay stage we can change the temporal overlap between the NIR and THz pulses (e.g., from  $-10$  ps to  $+10$  ps) and acquire a series of sideband spectra at selected values of  $\tau$ . The result of this procedure is shown in Fig. 3, where we present the intensities of both the  $\omega_{-1}$  and  $\omega_{-2}$  sidebands versus both the photon energy  $\hbar\omega$  and the relative delay time  $\tau$ . We observe that sidebands indeed appear only when the NIR and THz pulses temporally overlap. Given the fact that sidebands remain in the NIR part of the spectrum, we therefore arrive at the new method of measuring the temporal profile of the THz pulses using a Si photodetector.

Finally, we studied how the sideband intensities depend on the THz and NIR intensities. Figures 4(a) and 4(b) show

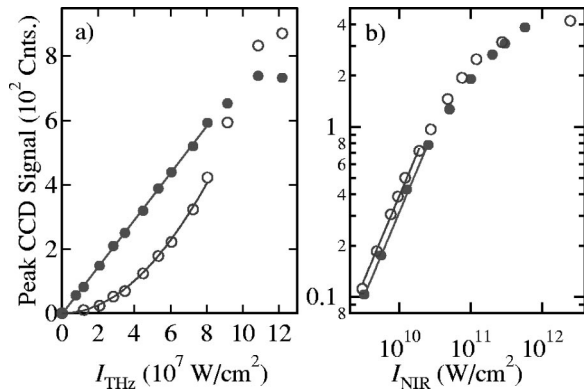


FIG. 4. (a) THz and (b) NIR intensity dependence of the THz intensity. The filled (open) circles represent the  $\omega_{-1}$  ( $\omega_{-2}$ ) sideband intensity. The solid curves are linear and quadratic fits to the data at low powers.

the sideband intensities at 160 K vs  $I_{THz}$  and  $I_{NIR}$ , respectively. At low  $I_{THz}$  the  $\omega_{-1}$  ( $\omega_{-2}$ ) sideband shows a linear (quadratic) dependence, consistent with a perturbative  $\chi^{(2)}$  ( $\chi^{(3)}$ ) process involving one (two) THz photons. However, at higher  $I_{THz}$  we observe a significant deviation from the perturbative behavior, which indicates the entrance into a strong THz field regime. A measure of the field strength at which such a deviation is expected is the ponderomotive potential, i.e., the time-averaged kinetic energy of an electron in an ac electric field.<sup>15</sup> For a laser field with strength  $E$  and frequency  $\omega$ , the ponderomotive potential is given by  $U_p = e^2 E^2 / 4m^* \omega^2$ , where  $m^*$  is the effective mass. At our highest THz intensity ( $\sim 1.2 \times 10^8$  W/cm $^2$ ),  $U_p$  is estimated to be about 180 meV, which is six times larger than the THz photon energy (30 meV), and thus it is reasonable to expect nonperturbative behavior to occur. Since only one NIR photon is involved in the generation process of either sideband, at low  $I_{NIR}$ , we see the expected linear dependence for both the  $\omega_{-1}$  and  $\omega_{-2}$  sidebands but it clearly saturates at higher intensities [see Fig. 4(b)]. Since NIR photons create real carriers above the bandedge ( $\hbar\omega_{NIR} \approx E_g$ ), free-carrier absorption of the THz radiation can result in the saturation of the sideband intensity. In addition, the population of the conduction band reduces the number of states that contribute to the sideband generation that are resonant to the fundamental (phase-space filling).

The experimental observation of the odd sideband implies the lack of inversion symmetry. The observed angular dependence on the incident beams suggests that the symmetry breaking is normal to the sample surface. While it is possible that the sample surface is playing a role via band-bending due to Fermi-level pinning and the presence of residual carriers, we expect such surface contributions to be small compared to the bulk (or intrinsic) contribution, i.e., the lack of inversion symmetry of the bulk GaAs crystal. Hence, we propose an explanation based on a bulk  $\chi^{(2)}$  consideration.

The second-order correction to the polarization induced by two radiation fields can be written as

$$P_i(\omega_1) = \sum_{jk} \chi_{ijk} E_j(\omega_{THz}) E_k(\omega_{NIR}), \quad (2)$$

where  $i, j, k$  denote the Cartesian coordinates,  $x, y, z$ . The second-order optical susceptibility tensor  $\chi_{ijk}$  is determined by the crystallographic symmetry of GaAs, which belongs to the  $\bar{4}3m$  crystal class, so there exist only three nonzero tensor elements:

$$\hat{\chi}^{(2)} = \begin{bmatrix} 0 & 0 & 0 & \chi^{(2)} & 0 & 0 \\ 0 & 0 & 0 & 0 & \chi^{(2)} & 0 \\ 0 & 0 & 0 & 0 & 0 & \chi^{(2)} \end{bmatrix}. \quad (3)$$

This reduces Eq. (2) to

$$P_i(\omega_1) = 2\chi^{(2)} \sum_{jk} E_j(\omega_{THz}) E_k(\omega_{NIR}). \quad (4)$$

Now, assuming that both beams propagate along the  $z$  direction, let us consider the dependence of the sideband generation on the sample orientation and the beam polarizations. It is easy to see that in the case of normal incidence and either parallel or perpendicular polarizations of the beams, the  $P_x$  and  $P_y$  components of the induced polarization  $P$  vanish and therefore no  $\omega_{-1}$  sideband is expected. However, if the sample is at 45 degrees with respect to the beams, the resulting  $P$  is perpendicular to the propagation direction and has the same absolute value for both polarization conditions. Therefore, one expects the bulk  $\chi^{(2)}$ -induced  $\omega_{-1}$  sideband to appear, which is in agreement with our observations.

In summary, we have performed THz sideband generation from bulk GaAs and observed new features. The sidebands appeared below the band gap where there are no states. We demonstrated a scheme to measure the temporal profile of

the THz pulses with a NIR detector. The THz power dependence clearly revealed a nonperturbative strong field regime. Finally, we detected an odd sideband, which has previously been observed only in an asymmetric quantum-well system where the inversion symmetry was intentionally broken. These observations are consistent with our theoretical consideration based on a bulk  $\chi^{(2)}$  model and provide significant new insight into the dynamics of THz driven semiconductors.

We gratefully acknowledge support from NSF Grant DMR-0049024, ONR N00014-94-1-1024, the Japan Science and Technology Corporation PRESTO Program, and the NEDO International Joint Research Grant Program. We thank Dr. K. Johnsen for useful discussions, Professor H. A. Schwettman for his support, and Professor H. Sugawara, Dr. M. Yoshita, Professor H. Akiyama, Dr. T. Kimura, J. M. Bakker, and J. Hayden for their assistance with the experiments.

\*Present address: Department of Physics, University of Utah, Salt Lake City, Utah 84112, Electronic address: maz@physics.utah.edu

†To whom correspondence should be addressed; URL: <http://www.ece.rice.edu/~kono>; Electronic address: kono@rice.edu

‡Present address: Lineup Technologies, Inc., 2329 S. Purdue Ave., Los Angeles, California 90064.

<sup>1</sup>W. Franz, Z. Naturforsch. A **13A**, 484 (1958).

<sup>2</sup>L.V. Keldysh, Zh. Éksp. Teor. Fiz. **34**, 1138 (1958) [Sov. Phys. JETP **7**, 788 (1958)].

<sup>3</sup>D.A.B. Miller, D.S. Chemla, T.C. Damen, A.C. Gossard, W. Wiegmann, T.H. Wood, and C.A. Burrus, Phys. Rev. Lett. **53**, 2173 (1984).

<sup>4</sup>S.H. Kwok, H.T. Grahn, K. Ploog, and R. Merlin, Phys. Rev. Lett. **69**, 973 (1992).

<sup>5</sup>J. Kono, M.Y. Su, T. Inoshita, T. Noda, M.S. Sherwin, S.J. Allen, and H. Sakaki, Phys. Rev. Lett. **79**, 1758 (1997).

<sup>6</sup>K. Johnsen, Phys. Rev. B **62**, 10 978 (2000).

<sup>7</sup>T. Inoshita and H. Sakaki, *Proceedings of the 24th International Conference on the Physics of Semiconductors*, edited by D. Gershoni (World Scientific, Singapore, 1999).

<sup>8</sup>K. Johnsen (unpublished).

<sup>9</sup>T. Inoshita, Phys. Rev. B **61**, 15 610 (2000).

<sup>10</sup>D.S. Citrin, Phys. Rev. B **60**, 13 695 (1999).

<sup>11</sup>C. Phillips, M.Y. Su, M.S. Sherwin, J. Ko, and L. Coldren, Appl. Phys. Lett. **75**, 2728 (1999).

<sup>12</sup>T. Inoshita, J. Kono, and H. Sakaki, Phys. Rev. B **57**, 4604 (1998).

<sup>13</sup><http://www.stanford.edu/group/FEL/>.

<sup>14</sup>A.H. Chin, O.G. Calderon, and J. Kono, Phys. Rev. Lett. **86**, 3292 (2001).

<sup>15</sup>A.H. Chin, J.M. Bakker, and J. Kono, Phys. Rev. Lett. **85**, 3293 (2000).